# Supporting information

## Three-Component Vesicle Aggregation Driven by Adhesion Interactions between Au Nanoparticles and Polydopamine-Coated Nanotubes

*Haibao Jin,[a] Yongfeng Zhou,[*,a,b] Wei Huang,[a] Yongli Zheng,[a] Xinyuan Zhu,[a,b] and Deyue Yan[a,b]*

*[a]School of Chemistry and Chemical Engineering, Shanghai Jiao Tong University, State Key Laboratory of Metal Matrix Composites, 800 Dongchuan Road, Shanghai 200240, China.*

*[b]Jiangsu Collaborative Innovation Center of Bio-medical Functional Materials, Jiangsu Key Laboratory of Biomedical Materials, College of Chemistry and Materials Science, Nanjing Normal University, Nanjing 210046, China*

## 1. Experimental section

### 1.1 Materials

HBPO-star-PEO was synthesized based on our previous reports through cationic ring-opening polymerization (CROP).[1,2] The polymer possessed the HBPO core with the molecular weight about 4,300 according to GPC and degree of branching (DB) of 38%. The number-average molecular weight ($M_n$) measured by GPC is about 8,500. Thus, the number-average degree of polymerization (DP) of the PEO arms is 2. Dopamine•HCl was purchased from Acros Organics. 2-Amino-2-hydroxymethyl-propane-1,3-diol (Tris) was purchased from Alfa Aesar. Hydrobromic acid (40%), sodium thiosulfate pentahydrate, sodium borohydride and other chemical reagents were purchased from Shanghai Chemical Reagent Co. and used as received.

### 1.2 Synthesis of thiol-modified hyperbranched polymers of HBPO-star-PEO-SHs

The synthesis process was performed according to the previous reported methods (Scheme S1).[3] In step 1, halogenating reaction was performed by using HBPO-star-PEO to react with hydrobromic acid (40%), forming a brominated polymer. In step 2, brominated polymer was further reacted with sodium thiosulfate pentahydrate to form the Bunte salt. In step 3, the thiol-modified hyperbranched polymer (HBPO-star-PEO-SH) was prepared through the reduction of the Bunte salt by using HCl as the reducing agent.

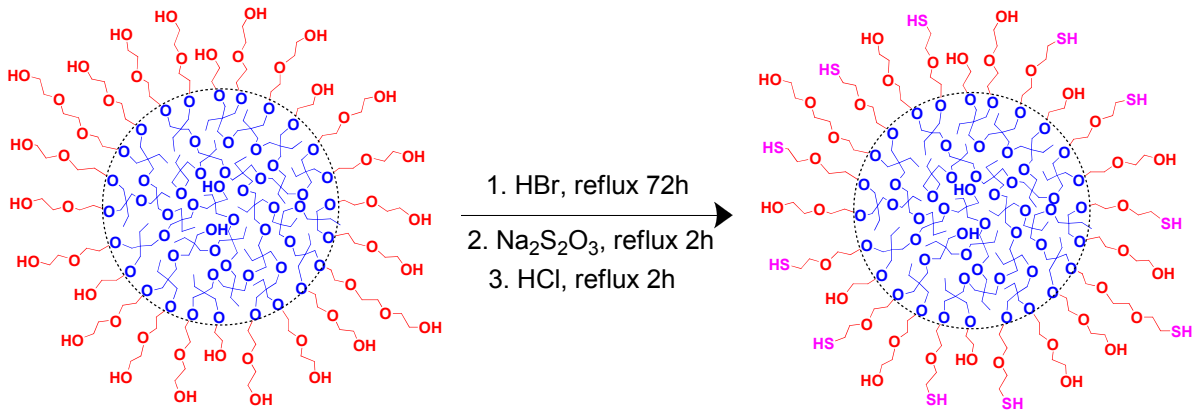


**Scheme S1.** Synthesis scheme of HBPO-star-PEO-SH. *Reagents and conditions*: (1) hydrobromic acid (40%), toluene, reflux, 72 h; (2) sodium thiosulfate pentahydrate, ethanol/water, reflux, 2 h; (3) 1M HCl, chloroform, reflux, 2 h.

### 1.3 Preparation of SBP@Au Composite

25 mg of HBPO-star-PEO-SH was dissolved in 5 mL of chloroform solvent for 30 min. Then, the solvent was evaporated to dryness, obtaining a polymers solid. 5 mL of distilled water at about 25 $^{o}$C was added with strong stirring. The appearance of turbidity in the solution indicated the formation of thiol-modified BPs. The final polymer concentration is 5 mg•mL$^{-1}$, and the thiol group concentration is approximately 8.6 mM. Following, 20 µL of $HAuCl_4$ aqueous solution (30 mM) was added into 2.5 mL of thiol-modified BPs solution. Then freshly prepared 0.1M $NaBH_4$ solution was added to the solution while strong stirring.

### 1.4 Preparation of WMCNTs@PDA

In a typical experiment, 100 mg of MWCNTs were added to 100 ml of deionized water, and the mixture was sonicated for 30 min. Dopamine•HCl (200 mg) and 120 mg of Tris were added. The resulting fine suspension was magnetically stirred at room temperature. After 12 hours, the suspension was centrifuged at 10000 rpm for 10 min, the supernatant was discarded and the remaining pellet was

washed with deionized water three times before finally drying the MWCNTs@PDA composite in a vacuum at 50 $^{o}$C.

### 1.5 Coassembly of SBP@Au composite with MWCNTs@PDA

6 mg of MWCNTs@PDA was dispersed in the 20 mL of water by 5 minutes sonication. 2 mL such soltuion and 2 mL of SBP@Au composite solution were mixed together. 6 mg of Tris was added to adjust the pH 8.5, stirring for 24 hours.

## 2. Instruments and measurements

**2.1 NMR measurement.** $^{1}$H NMR was performed on a Varian Mercury Plus 400-MHz spectrometer using deuterated dimethyl sulfoxide (DMSO-d6) as solvents at 20 $^{o}$C, and tetramethylsilane (TMS) was used as the internal reference.

**2.2 Optical and Fluorescent microscope (OM and FM).** The morphologies of the vesicles were observed by optical microscopy microscope on a Leica DM4500 B. For the microscope observation, the aqueous solution was dropped onto a glass slide and then observed directly under the microscope.

**2.3 Scanning electron microscope (SEM).** SEM experiments were performed on JEOL 7401F field emission scanning electron microscope, with an accelerating voltage 5 kV. The samples were prepared by dropping a small drop of the polymer solution onto silicon wafer, and then quickly frozen by liquid nitrogen. Lyophilization was used to remove solvent water instead of evaporating at room temperature for a small disturbance of the sample morphologies. Then, the sample without coating with Au nanoparticles was sputter-coated with a homogeneous thin gold layer for charge dissipation during the SEM imaging.

**2.4 Transmission electron microscopy (TEM).** TEM results were obtained on a JEM-2010/INCA OXFORD instrument operating at an accelerating voltage of 200KV or on a FEI Tecnai G2 Spirit Biotwin instrument operating at an accelerating voltage of 120KV. For TEM measurement, a small drop

of the polymer solution was placed onto 400 mesh copper grids coated with Parlodion film stabilized with vacuum evaporated carbon, and then quickly frozen by liquid nitrogen. Lyophilization was used to remove solvent water instead of evaporating at room temperature for a small disturbance of the sample morphologies.

**2.5 Ultraviolet-visible absorption spectrum (UV/Vis).** UV-Vis spectra were recorded on a Lambda 750S spectrometer, made by Perkin Elmer, Inc., USA. All the samples were measured at the room temperature. The scanning range of the spectra was form 400 nm to 700 nm with 2 nm slit. The scanning rate was set at 480 nm/min.

**2.6 Thermalgravimertic analysis (TGA).** TGA experiments were performed on PerkinElmer TGA 7, made by Perkin Elmer, Inc., USA. All the samples were measured under the oxygen atmosphere.

**2.7 Fourier transform infrared spectra (FTIR).** Fourier transform infrared (FTIR) spectra were recorded on a PE Paragon 1000 spectrometer. All the samples were prepared by dispersion in KBr pellets.

## 3. Characterizations

### 3.1 The morphology characterization of BPs from HBPO-star-PEOs

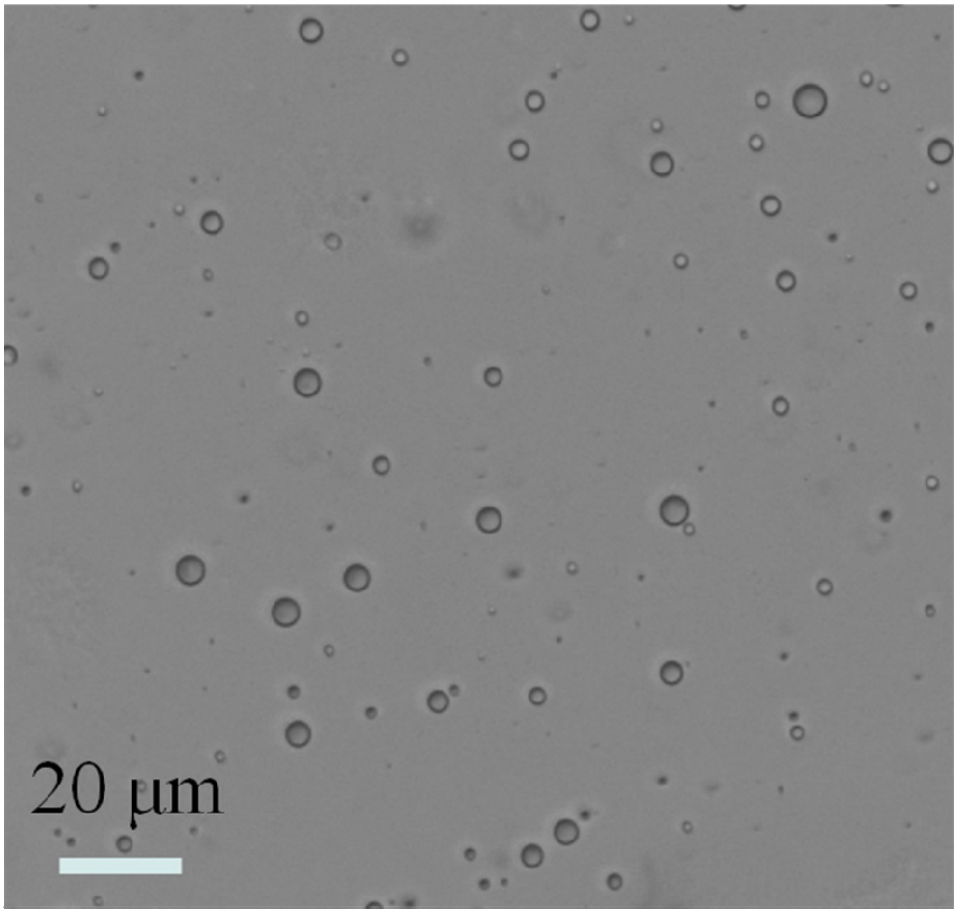


**Figure S1.** Optical micrograph of BPs obtained from the self-assembly of HBPO-star-PEOs.

### 3.2 Synthesis of HBPO-star-PEO-SHs

The $^1$H NMR spectra of HBPO-star-PEOs with $DP_{arm}$=2 and HBPO-star-PEO-SHs are shown in Figure S2. Comparing with the $^1$H NMR spectrum of HBPO-star-PEOs, new proton signals appeared at 1.97 (proton k) in the spectrum of HBPO-star-PEO-SHs, which confirmed that thiol groups was grafted onto HBPO-star-PEO successfully. The conversion of hydroxyl groups calculated by comparing the integral of peaks k with that of peak A (0.82 ppm) according to the formula ($3S_k/S_A$) was about 36%.

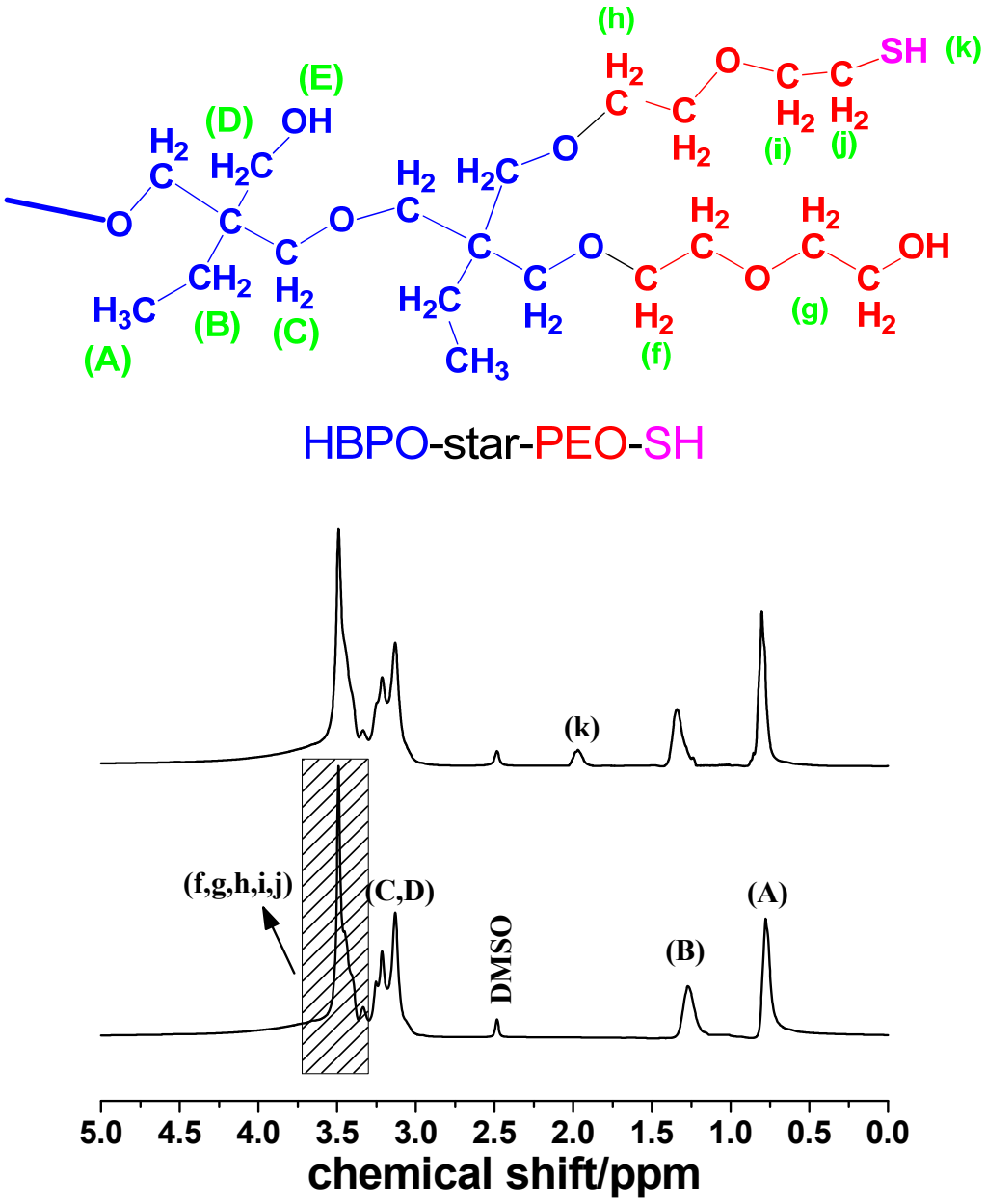


**Figure S2.** $^1$H NMR spectra of HBPO-star-PEO-SHs (up) and HBPO-star-PEOs (down).

### 3.3 Morphology characterizations of SBPs and SBP@Au composites

A dye encapsulation experiment was performed to prove the hollow lumens of SBPs. When a drop of rhodamine B aqueous solution (1 wt%) was added into the vesicle solution, the vesicle lumens were totally encapsulated with the red rhodamine B dyes (green arrow, Figure S3a) according to the optical phase-contrast microscopy. Such a result clearly supports a hollow lumen structure in the SBPs. For the fluorescent micrograph of pyrene-labeled SBPs (inset of Figure S3a) clearly illustrates the hollow interior of vesicular morphology, as evidenced by a significant decrease in fluorescence intensity toward the center of the spheres. Besides, the collapsed circular particles observed by SEM (Figure S3b) agreed well with the optical microscope results in structure and size.

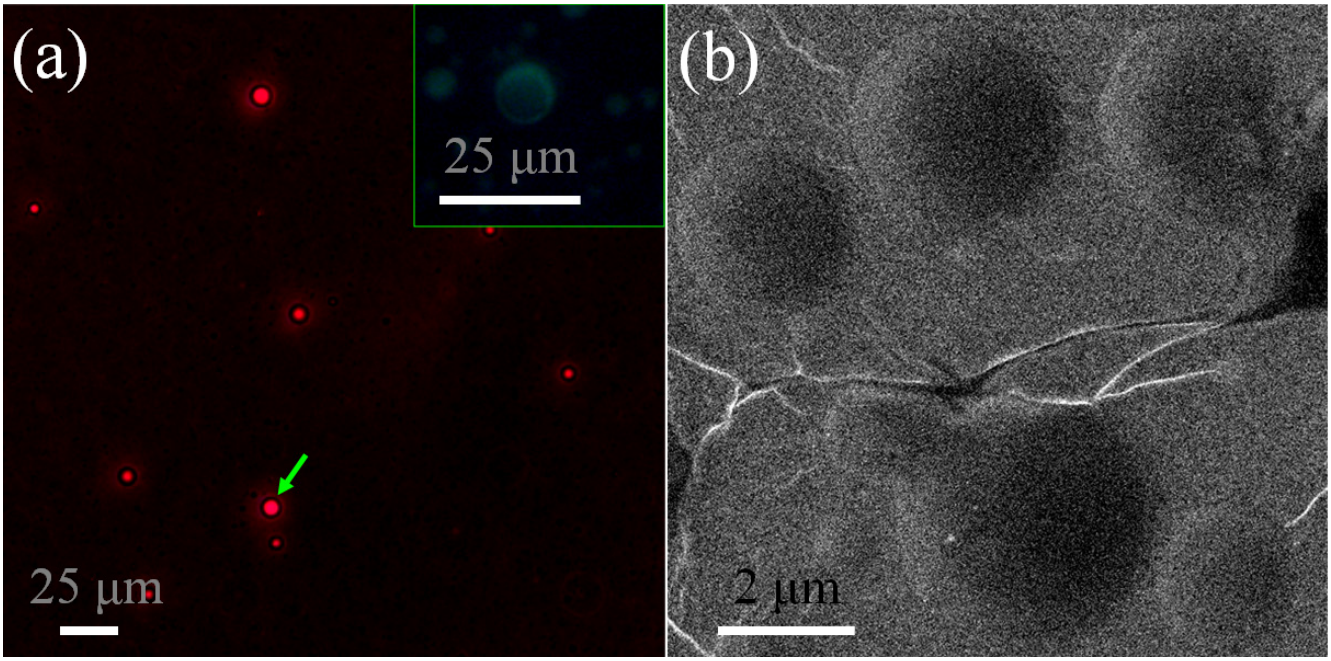


**Figure S3.** Morphology characterizations of SBPs. (a) The Optical phase-contrast micrograph of the vesicles encapsulated with red rhodamine dyes as well as the fluorescent image (inset); (b) The SEM image of the dried vesicles.

Figure S4a shows the optical micrograph (bright field) of the SBPs self-assembled from HBPO-star-PEO-SHs. After the reduction of $HAuCl_4$, the spherical vesicular structure and the vesicle size were kept (Figure S4b). The vesicles seemed to have a denser and thicker membrane according to the darker boundary of the vesicles in optical microscope, which is probably due to the coat of Au nanoparticles onto the surface of the obtained SBP@Au composites.

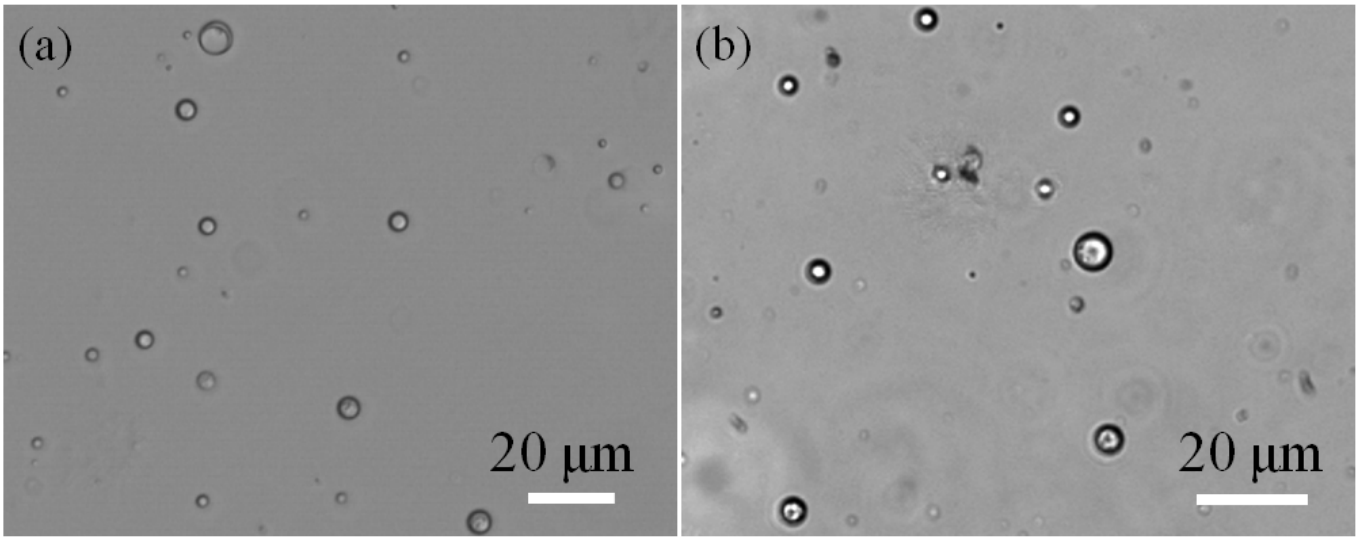


**Figure S4.** (a) Optical micrograph of SBPs obtained from the self-assembly of HBPO-star-PEO-SH, (b) SBP@Au composite formed through the reduction of $HAuCl_4$ onto the membrane of SBPs.

### 3.4 Characterizations of vesicle aggregates in a dried state

Vesicle aggregates were characterized by the optical microscope (OM), scanning electron microscope (SEM) and transmission electron microscope (TEM). Figure S5a showed the vesicle aggregate from SBPs@Au with MWCNTs@PDA at Tris buffer (pH=8.5) observed by the OM (bright field), indicating it was composed of densely packed vesicles. After the evaporation of water, the structure and morphology of the aggregate were mostly kept (Figure S5b).

SEM could give us some details for the connection of vesicle aggregates. As shown in the Figure S5c, it is the magnified location of Figure 3d in the main manuscript. It is found that there are many multiwalls carbon nanotubes uniformly dispersed on the surfaces or boundaries of the vesicle aggregates.

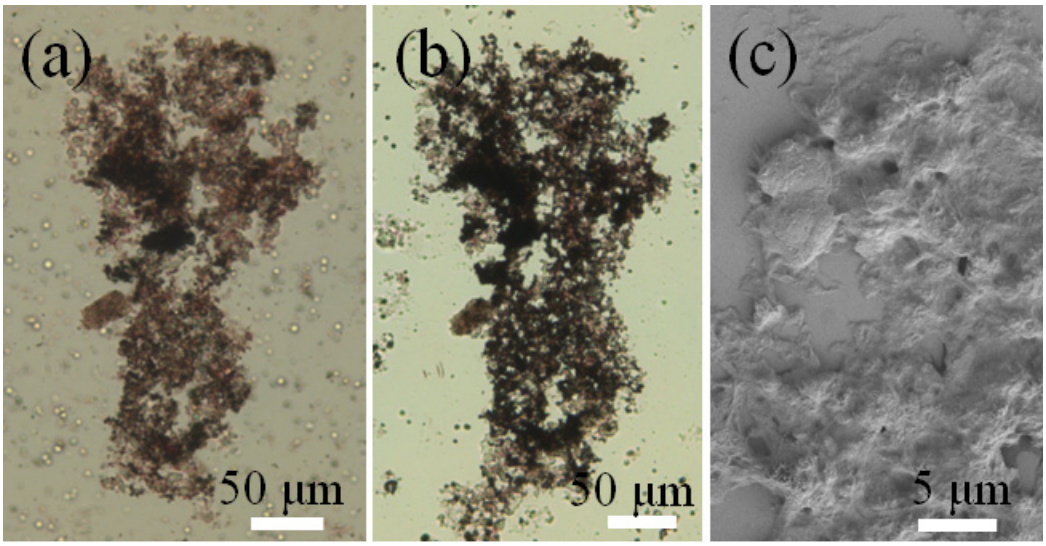


**Figure S5.** Optical micrograph of vesicle aggregates obtained through interconnecting SBP@Au by MWCNTs@PDA. (a) The vesicle aggregate in water (the same sample as that in Figure 3b of main text) under bright field; (b) The same vesicle aggregate in a dried state under bright field; (c) The magnified image of Figure 3d in the manuscript.

TEM (JEM-2010/INCA OXFORD, accelerating voltage 200 kv) was used to discern the connection method between SBPs@Au and MWCNTs@PDA. Figure S6 shows the TEM images of some vesicle oligomers, which supports that the vesicles are connected by the carbon nanotubes. In the magnified TEM images (Figures S6b and S6d), it can be clearly seen that Au nanoparticles were coated on the PDA layers of MWCNTs@PDA. Besides, the EDX measurement of vesicle aggregate (Figure S6e) shows there are gold, sulfur, carbon, and oxygen elements distributed in these aggregates. These results indicate that the vesicles are connected together by the carbon nanotubes driven by the adhesion interaction between Au nanoparticles on the vesicles and PDA shells coated on the nanotubes.

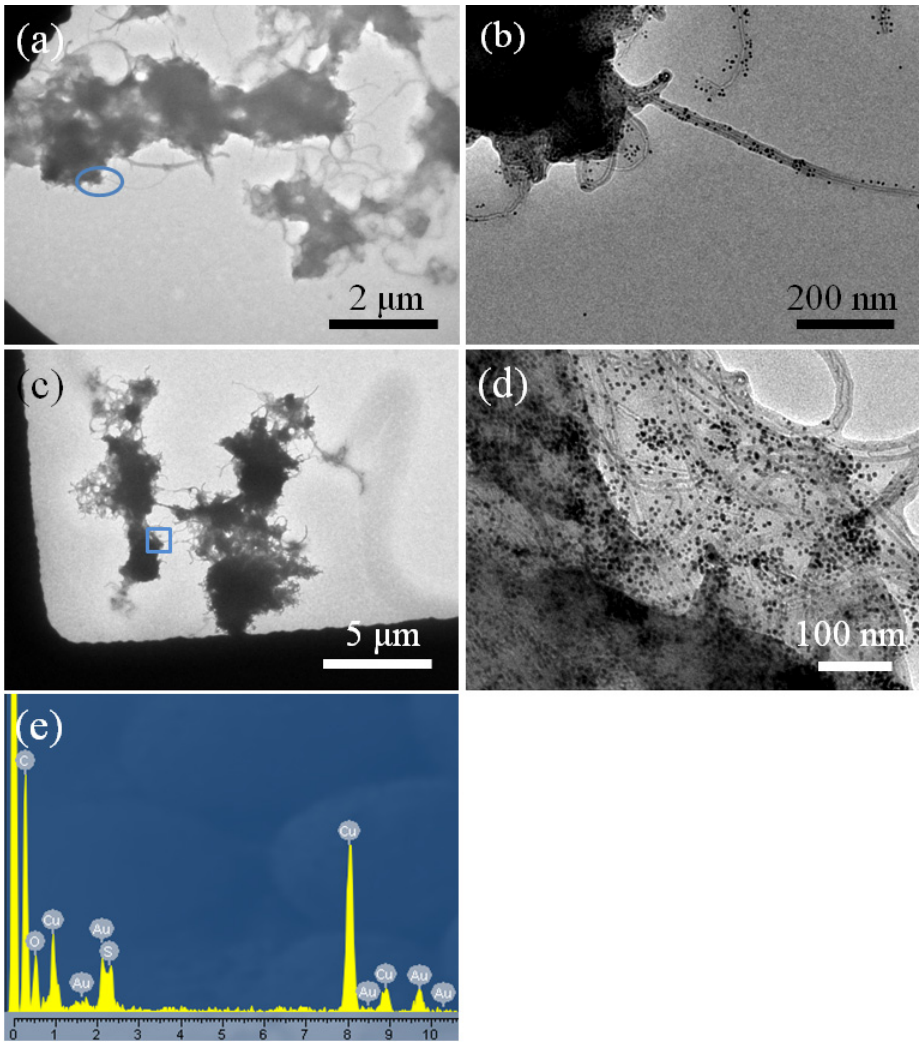


**Figure S6.** The TEM images of the vesicle aggregates from SBPs@Au and MWCNTs@PDA at an accelerating voltage of 200 kv. Image (b) is a magnified view of image (a) as indicated by the blue circle; Image (d) is a magnified view of image (c) as indicated by the blue square; (e) The EDX analysis.

To avoid the decomposition of organic materials under high accelerating voltage of 200 kv, the vesicle aggregates were further characterized by the TEM operated at an accelerating voltage of 120 kv (FEI Tecnai G2 Spirit Biotwin instrument). The results are shown in Figure S7, which are almost the same as those at an accelerating voltage of 200 kv (Figure S6). There are many MWCNTs@PDA existing on the vesicular surfaces or adjacent spaces, and the samples are too thick to be penetrated by electron beam. Thus, the vesicles are black and their detailed inner structure is difficult to be discerned. In fact, no clear decomposition process of the vesicle aggregates was observed during the TEM measurements under high accelerating voltage either at 200 kv or at 120 kv. The vesicles in the aggregate looked irregular and highly deformed (Figure 3f in the main text, Figures S6 and S7 in the supporting information), probably due to the solvent evaporation during the TEM sampling process.

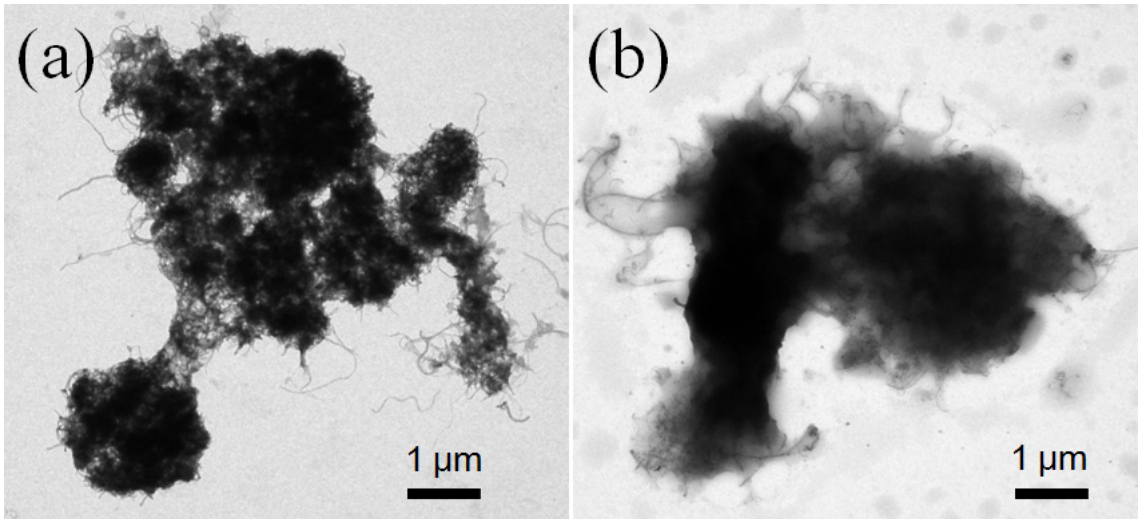


**Figure S7.** The TEM images of the vesicle aggregates obtained through interconnecting SBPs@Au by MWCNTs@PDA at an accelerating voltage of 120 kv.

The UV/Vis spectra were also used to trace this vesicle aggregation process (Figure S8). For SBP@Au solution, the surface plasmon resonance (SPR) peak around 570 nm appeared in the spectrum, due to the strong inter-nanoparticles coupling between adjacent gold nanoparticles. While for the vesicle aggregates from SBPs@Au and MWCNTs@PDA, the SPR peak showed a blue shift, shifting from 570 nm to 528 nm. Such a blue-shift is attributed to decrease of inter-nanoparticle coupling between adjacent AuNPs induced by the adhesions of AuNPs onto PDA layers of MWCNTs@PDA (as proved by the TEM images of Figure 3f and Figures S6-S7 in the supporting information), which provides further evidence to support the interconnection of SBPs@Au by MWCNTs@PDA to form aggregates.

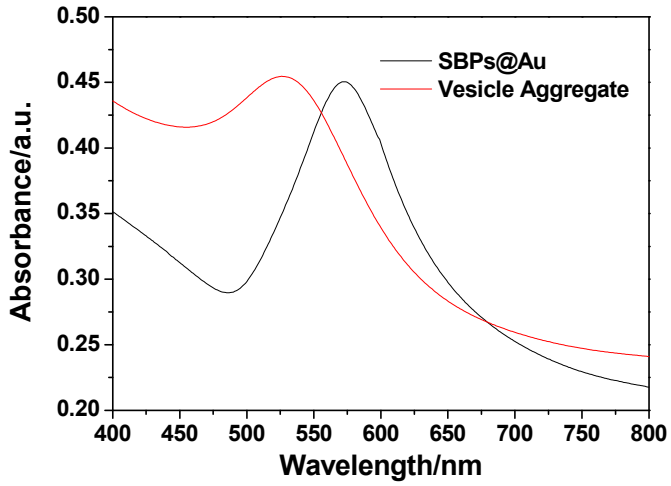


**Figure S8.** UV/Vis spectra of SBPs@Au and vesicle aggregates from SBPs@Au and MWCNTs@PDA.

### 3.5 The control experiments to indicate the adhesion interaction between Au-nanoparticles and PDA-coated MWCNTs

For the first control experiment, Au nanoparticles were firstly prepared through the reduction of $HAuCl_4$ by sodium borohydride (Figure S9a) in the presence of block copolymer of PEG-*b*-PDMAEMA (PDMAEMA is abbreviated from poly(2-(dimethylamino) ethyl methacrylate)).[4] The average size of Au nanoparticles was about 8.1 nm according to the TEM images (Figure S9a) . The adhesion experiment was performed by mixing Au nanoparticles and MWCNTs@PDA together at Tris buffer (pH=8.5). After 24 hours, the mixture was characterized by the TEM. It was found that Au nanoparticles were successfully loaded onto the PDA layer of MWCNTs@PDA (Figure S9b), which proves the adhesion interaction between Au-nanoparticles and PDA layers coated on the surface of CNTs.

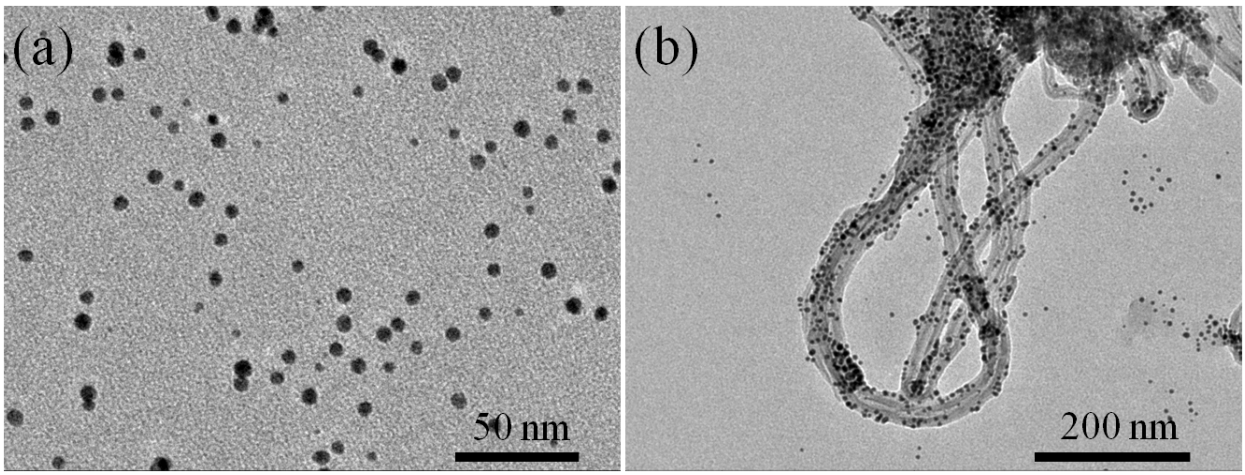


**Figure S9.** (a) Au nanoparticles prepared through the reduction of $HAuCl_4$; (b) MWCNTs@PDA@Au prepared by mixing Au nanoparticles and MWCNTs@PDA at Tris buffer (pH=8.5).

For the second control experiment, we mixed SBPs@Au and pristine MWCNTs together. At the beginning, both SBPs@Au and pristine MWCNTs (white arrows) were uniformly dispersed in the solution (Figure S10a). After 24 hours, no vesicle aggregates were observed while some pristine MWCNTs were aggregated and precipitated (green arrows) due to the strong hydrophobicity (Figure S10b).

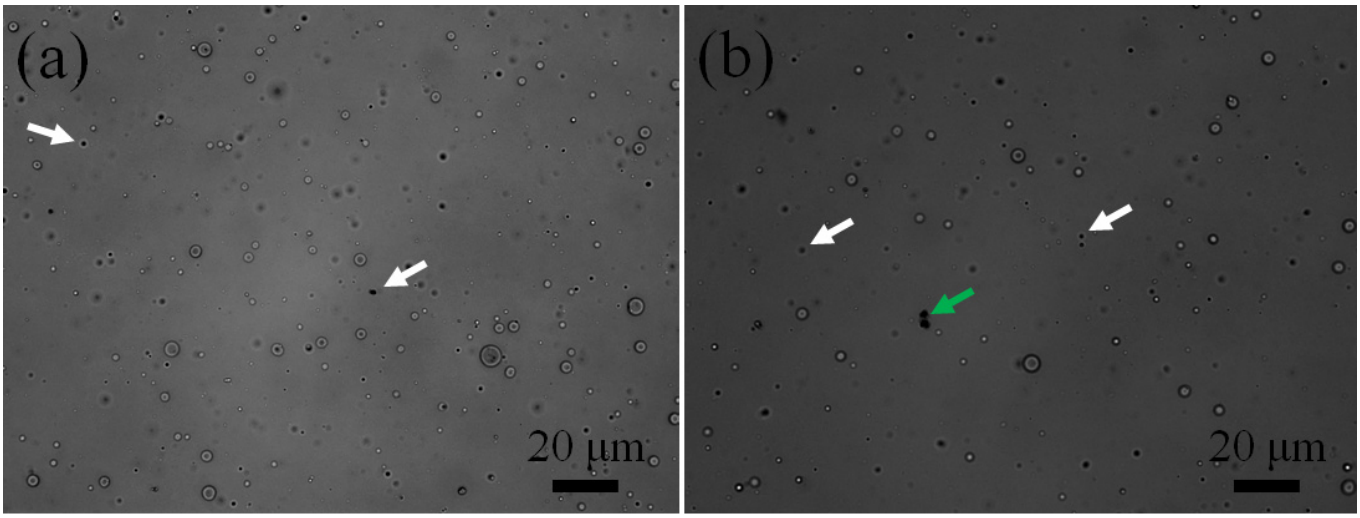


**Figure S10.** Optical micrographs after mixing SBPs@Au and pristine MWCNTs together with different times of 0 h (a) and 24 h (b).

### 3.6 Statistical analyses of vesicle diameters

The vesicle size before and after aggregation were analyzed (Figure S11), which shows that there are no clear size changes in the aggregation process. In other words, fusion events are successfully prohibited in the present work.

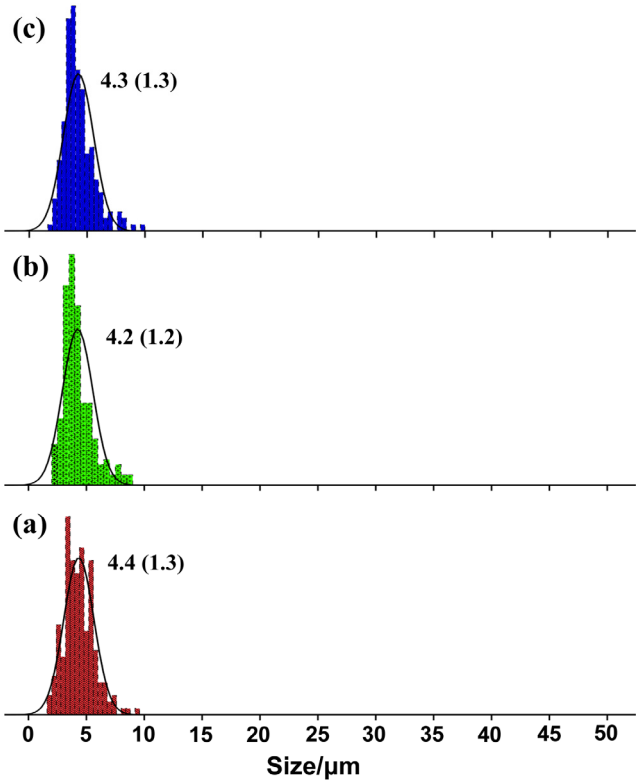


**Figure S11.** Statistical size distributions of the vesicles from: (a) SBP@Au; (b) vesicle aggregate after mixing for 24 h; and (c) vesicle aggregate after incubation for 72 h. The numbers above each histogram are the average vesicle diameters with the standard deviations in parentheses; 200 vesicles were analyzed for each size distribution.

References and Notes

1. Y. F. Zhou, D. Y. Yan, *Angew. Chem. Int. Ed.* **2004**, *43*, 4896.

2. Y. F. Zhou, D. Y. Yan, W. Y. Dong, Y. Tian, *J. Phys. Chem. B* **2007**, *111*, 1262.

3. H. Wolf, H. Ringsdorf, E. Delamarche, T. Takami, H. Kang, B. Michel, C. Gerber, M. Jaschke, H. J. Butt, E. Bamberg, *J. Phys. Chem.* **1995**, *99*, 7102.

4. L. Bromberg, S. Deshmukh, M. Temchenko, L. Iourtchenko, V. Alakhov, C. Alvarez-Lorenzo, R. Barreiro-Iglesias, A. Concheiro, T. A. Hatton, *Bioconjugate Chem.* **2005**, *16*, 626.